Environ. Sci. Technol. **1997**, *31*, 689−696

Effects of Temperature on Trichloroethylene Desorption from Silica Gel and Natural Sediments. 1. Isotherms

CHARLES J. WERTH† AND MARTIN REINHARD*

Environmental Engineering and Science, Department of Civil Engineering, Stanford University, Stanford, California 94305-4020

Aqueous phase isotherms were calculated from vapor phase desorption isotherms measured at 15, 30, and 60 °C for trichloroethylene on a silica gel, an aquifer sediment, a soil, a sand fraction, and a clay and silt fraction, all at 100% relative humidity. Isosteric heats of adsorption ($Q_{st}(q)$) were calculated as a function of the sorbed concentration, q, and examined with respect to the following mechanisms: adsorption on water wet mineral surfaces, sorption in amorphous organic matter (AOM), and adsorption in hydrophobic micropores. Silica gel, sand fraction, and clay and silt fraction 60 °C isotherms are characterized by a Freundlich region and a region at very low concentrations where isotherm points deviate from log-log linear behavior. The latter is designated the non-Freundlich region. For the silica gel, values of $Q_{st}(q)$ (9.5−45 kJ/mol) in both regions are consistent with adsorption in hydrophobic micropores. For the natural solids, values of $Q_{st}(q)$ in the Freundlich regions are less than or equal to zero and are consistent with sorption on water wet mineral surfaces and in AOM. In the non-Freundlich regions, diverging different temperature isotherms with decreasing q and a $Q_{st}(q)$ value of 34 kJ/mol for the clay and silt fraction suggest that adsorption is occurring in hydrophobic micropores. The General Adsorption Isotherm is used to capture this adsorption heterogeneity.

Introduction

Recent efforts to enhance subsurface transformation and transport rates for volatile organic chemicals have examined the effects of elevated temperature (*1, 2*). These efforts have been carried out with little knowledge of the mechanisms controlling and the effects of temperature on intragranular transport processes. Since intragranular transport processes affect, and can control, transformation and transport rates (*3*−*9*), elucidation of the mechanisms controlling them is paramount to determining the efficacy of *in-situ* thermal remediation technologies. As a first step toward this end, it is necessary to understand sorption equilibria. This involves characterizing the types and the capacity of potential sorption sites within natural grains.

Soil and sediment grains possess both compositional and structural variability. Compositional variables include types and amounts of minerals and organic matter. Structural variables include surface area and pore size. Pore sizes fall into three classifications based on adsorbate behavior: macropores (<500 Å), mesopores (20−500 Å), and micropores (<20 Å) (*10*). Surface area and porosity characteristics are determined by the aggregation of minerals and organic matter. Overall soils and sediments are thought be hydrophilic, with adsorptive displacement by water of organics causing greater than 100-fold decreases in the amount of organic sorbed over that on dry soil (*7, 11*). Mineral surfaces are primarily hydrophilic (*12*) and are thought to make up the majority of surface area and porosity. Soil organic matter (SOM) is hydrophobic and is thought to be distributed within and on mineral aggregates. SOM has been proposed to consist of "soft" amorphous humic materials and "hard" increasingly condensed microcrystalline materials (*13, 14*). Therefore, crystalline-like micropores may be formed from both mineral surfaces and hard SOM.

From the observed variability in natural solids, several mechanisms are hypothesized to contribute to organic chemical sorption from the vapor phase. These mechanisms are adsorption at the air−water interface, partitioning to intragranular water, absorption in amorphous organic matter (AOM), adsorption on water wet mineral surfaces, and adsorption in micropores. For sorption from the aqueous phase, only the later three mechanisms must be considered.

Sorption mechanisms are characterized by different free energies. Thus, different mechanisms can dominate sorption at different contaminant loadings. Sorption mechanisms are also characterized by different heats of adsorption. Consequently, temperature can affect sorption at one contaminant loading more than at another contaminant loading. It is the intent of this paper to investigate the mechanisms controlling sorption equilibria by comparing isosteric heats of adsorption ($Q_{st}(q)$) calculated from different temperature aqueous phase isotherms with published heats of adsorption for similar compounds in model solids. Temperature effects are distinguished from hysteresis effects before computing $Q_{st}(q)$ values. Aqueous phase isotherms are calculated from vapor phase desorption isotherms measured at 15, 30, and/or 60 °C for trichloroethylene (TCE) on a silica gel and four natural solids at 100% RH.

Theory

Local Isotherms. A single 'local' isotherm describes partitioning when one mechanism controls sorption. The simplest local isotherm is the linear isotherm shown in eq 1.

$$q_l = K_{d,aq} C_{aq} \tag{1}$$

Use of the linear isotherm assumes that all sorption sites have an equal affinity for the sorbate and that $K_{d,aq}$ is independent of the aqueous phase concentration. Linear isotherms have been used to describe sorption to water wet sediments over a limited concentration range (*3*) and partitioning to soils rich in organic matter (*15*−*17*). Partitioning to organic matter exceeds adsorption on water wet mineral surfaces in organic rich soils. McCarty et al. (*18*) postulated that partitioning to organic matter dominates sorption if the fraction of organic carbon (f_{oc}) exceeds a critical fraction defined as

$$^*f_{oc} = \frac{S}{200 K_{ow}^{0.84}} \tag{2}$$

Equation 2 was derived from regressions using silica gel and organic matter and caution must be used in its application to natural solids.

* Author to whom all correspondence should be addressed. Fax: (415)725-3162; e-mail: reinhard@ce.stanford.edu.

†Present address: Department of Civil Engineering, University of Illinois at Urbana−Champaign, Urbana, IL 61801.

S0013-936X(96)00230-1 CCC: $14.00

A slightly more complex local isotherm is the Langmuir isotherm shown in eq 3 (*19*).

$$q_l = \frac{bC_{aq}q_{l,s}}{1 + bC_{aq}} \quad (3)$$

Use of the Langmuir isotherm assumes that sorption occurs on a finite number of identical sites. The Langmuir isotherm has been successfully applied to organic sorption on microporous solids (*20*−*22*).

General Adsorption Isotherm. To simulate sorption on soils and sediments, a model that accounts for several different sorption mechanisms is required. The General Adsorption Isotherm (GAI), shown in eq 4, is one such model (*23* and references therein).

$$\Theta = \frac{q}{q_s} = \sum_{n=1}^{N}\left(\int_0^{\infty} \phi_n(\epsilon_{aq})\theta_{l,n}(\epsilon_{aq})\, d\epsilon_{aq}\right) \quad (4)$$

The overall adsorption isotherm, Θ, is obtained by adding together the contribution from each of the N sorption mechanisms. A local isotherm, $\theta_l(\epsilon_{aq}) = q_l/q_{l,s}$, is used to account for each sorption mechanism, and each local isotherm is integrated over the normalized distribution of free energies, $\phi(\epsilon_{aq})$, that characterize sorption via that particular mechanism. For sorption from the aqeuous phase to soils and sediments, three mechanisms are believed to contribute to uptake ($N = 3$). Hence, there are three local isotherms, each with its own $\phi(\epsilon_{aq})$. The advantage of using the GAI is that it can simulate adsorption up to any level of complexity.

The Freundlich isotherm (*24*), shown in eq 5, is a common form of the GAI used to model partitioning to soils and sediments.

$$q = K_{F,aq}C_{aq}^{1/n} \quad (5)$$

In the gas phase, the Freundlich isotherm can be derived via first principles from the GAI with eq 4 and with $\phi(\epsilon_{aq}) = \alpha e^{-\epsilon_{aq}/RT}$ (*22*). In the liquid phase, the Freundlich equation is empirical. The Freundlich exponent $1/n$ is an indicator of sorption heterogeneity. When $1/n < 1$, a distribution of sites is present, and sorbates sorb to higher energy sites in order of decreasing aqueous phase concentration. Values of $1/n < 1$ have been observed for organic contaminant sorption onto water wet soils and sediments (*3, 5, 13, 25*−*27*), onto water wet silica gel (*5, 14*), and onto aqueous phase organic matter (*14*). Using TCE and the same solids examined in this study, Farrell and Reinhard (*5*) found the magnitude of $1/n$ could not be correlated to surface area or mesoporosity but might be inversely related to the amount of microporosity.

Data in this study will be analyzed with Freundlich isotherms where applicable. A different form of the GAI will be proposed to capture deviations from Freundlich behavior.

Hysteresis Effects. In the absence of hysteresis, the sorbed-aqueous equilibrium value, K_{aq}, is a function of the sorbed concentration, q, and the temperature, T. In the presence of hysteresis, K_{aq} is also a function of the initial q, which is a function of the initial relative vapor pressure $(P/P_s)_i$ (*5*). For sorption to water wet mineral surfaces, hysteresis has not been observed. However, equilibrium hysteresis has been observed for sorption to sediments high in organic matter ($f_{oc} > *f_{oc}$) (*5, 28*) and for adsorption in micropores (*29, 30*).

Temperature Effects. $Q_{st}(q)$ controls the effects of T on isotherms. In the absence of hysteresis, $Q_{st}(q)$ can be calculated at a given q with the integrated form of the van't Hoff equation:

$$Q_{st}(q) = R \ln (K_{aq}(q,T_2)/K_{aq}(q,T_1))(1/T_2 - 1/T_1)^{-1} \quad (6)$$

Values of $Q_{st}(q)$ are positive for exothermic adsorption and negative for endothermic adsorption. Three representative cases are identified for this paper: (1) $Q_{st}(q)$ equals zero [$K_{aq}(q,T_2) = K_{aq}(q,T_1)$] and different temperature isotherms coincide; (2) $Q_{st}(q)$ is positive [$K_{aq}(q,T_2) > K_{aq}(q,T_1)$; $T_2 < T_1$] over the entire q range and different temperature isotherms are separated and parallel; (3) $Q_{st}(q)$ is positive at low q values and decreases with increasing q, resulting in converging different temperature isotherms with increasing q.

Partitioning to AOM. TCE partitioning to AOM is driven by the hydrophobic effect (*31, 32*). The $Q_{st}(q)$ value for TCE partitioning to AOM can be correlated to the heat of phase transfer for TCE from water to its own pure phase. Following the method of Ben-Naim (*33*), the ΔG of phase transfer for TCE can be computed from eq 7 and varies by less than 4 kJ/mol between 15 and 60 °C.

$$\Delta G = RT\,(-\ln (H_c) + \ln (P_s/\rho_{TCE})) \quad (7)$$

As a result, the equilibrium distribution coefficient ($K = \exp(-\Delta G°/RT)$) changes <30% and the heat of phase transfer is <5 kJ/mol. Noll measured a similar $Q_{st}(q)$ value (1.37 kJ/mol) for aqueous phase benzene on a hydrophobic silica gel (C_{18}-SiO_2). Thus, $Q_{st}(q)$ values are expected to be low in AOM.

Adsorption on Water Wet Mineral Surface. Mineral surfaces are primarily hydrophilic (*12*). Water wet mineral surfaces are relatively low energy sites characterized by small $Q_{st}(q)$ values. Goss et al. (*12*) reported vapor phase heats of adsorption for volatile organics onto water wet mineral surfaces to be less than heats of condensation; Noll (*34*) measured $Q_{st}(q)$ values <0.157 kJ/mol for aqueous benzene on silica gel surfaces at 25 °C. Thus, for both partitioning to AOM and sorption to water wet mineral surfaces, isotherms are expected to coincide.

Adsorption in Micropores. Sorption behavior and temperature effects in soil and sediment micropores are expected to be similar to those in zeolite micropores. In zeolite micropores, temperature effects are a function of micropore hydrophobicity and pore width. Organics preferentially adsorb in hydrophobic micropores (*35, 36*), and water preferentially adsorbs in hydrophilic micropores (*37*). Hence, organic contaminants are not expected to displace water from hydrophilic micropores and only hydrophobic micropores are considered. Kaneko et al. (*38*) measured $Q_{st}(q)$ values near 27 kJ/mol for adsorption of nitrobenzene, benzoic acid, and phenol from water to hydrophobic microporous activated carbon fibers. Stach et al. (*39*) found that, for hydrophobic micropores decreasing from 22 and 5 Å in width, heats of adsorption for *n*-decane vapor rose exponentially from ~55 to 120 kJ/mol. Sorption energy also increases with decreasing micropore width (*40*). Hence, $Q_{st}(q)$ values for adsorption in hydrophobic micropores are large, and they increase with decreasing concentration when micropores having different widths are present. For a heterogeneous solid with a range of micropore characteristics (geometry and polarity), different temperature isotherms will exhibit different slopes and will converge toward higher concentrations.

Experimental Section

Sorbate and Sorbent Characterization. TCE was the only sorbate used in this study. It was used as a model sorbate because it displays characteristics typical of many hydrophobic volatile organic contaminants. It is also a common soil and groundwater contaminant (*41*−*43*). Properties of TCE used here are the saturation vapor pressure (P_s) and the Henry's constant (H_c). Gossett's (*44*) relationship was used to calculate H_c for TCE at 15 and 30 °C. This relationship was verified up to 45 °C. The value of H_c at 60 °C was measured using the modified EPICS method (*44*) and was 1.5(−). Values of P_s at 15, 30, and 60 °C were calculated from the Antoine equation (*45*).

One model and four natural sorbents were used in this study. The silica gel is the model sorbent and was chosen because it contains no measurable organic matter and a measurable amount of microporosity. The natural solids were chosen because they possess a range of characteristics allowing mechanistic comparisons between solids. Solid used were at 100% RH because much of the vadose zone is at 100% RH and sorption mechanisms in water saturated sediments are similar (*5*, and references therein). Relevant solid characteristics are shown in Table 1. In addition to the previously published characteristics (*5*): 30 °C isotherm values, surface area, natural organic matter content, intra-aggregate mesopore size distribution, and mean particle size; the water loading at 15 and 60 °C, the air−water interfacial area to water volume ratio, and the micropore volume are shown.

Desorption Isotherms. The methods used here to measure desorption isotherms are those used by Farrell (*46*), with slight modifications. Briefly, stainless steel columns (25 cm × 9 mm i.d.) were filled with soil and equilibrated to 100% RH at the temperature to be examined. The columns were then purged with water-saturated organic vapor until the effluent flux, as measured by a flame ionization detector (FID) mounted on an HP 5890 gas chromatograph (GC), was constant and equal to the influent flux. At this point, the columns were capped and allowed to equilibrate for at least 2 weeks and usually 1 month. After equilibration, the columns were purged with water-saturated nitrogen for 2−20 min, recapped, and allowed to re-equilibrate. The maximum constant effluent flux during a purge represented an isotherm point. This cycle continued until the column flux dropped to near the detection limit of the FID. Remaining TCE was removed by heating the columns to 180 °C while purging them with nitrogen and trapping the effluent on a column of Tenax (Alltech) adsorbent. The trapped organic was then desorbed by a Tekmar dynamic headspace concentrator and analyzed with a GC equipped with a photoionization detector (PID). This technique allows desorption isotherms to be measured for up to 5 orders of magnitude in vapor phase concentration.

Aqueous phase isotherms were calculated from vapor phase isotherms with

$$K_{aq}(q) = K_v(q_v)H_c - W_{sp} \qquad (8)$$

Use of this equation assumes that adsorption at the air−water interface was negligible. Karger et al. (*47*) found 21% of sorbed 1,2-dichloroethane was adsorbed at the water surface−vapor interface of silica when the water surface−vapor interface area to water volume ratio was 5 m^2/g. Ratios much less than this indicate that adsorption via this mechanism is not significant. Values of this ratio in Table 1 are 0.02 m^2/g. However, for the Livermore clay and silt fraction, only the upper limit of the particle diameter is known (*5*). Hence, this ratio could be much higher than reported.

Precision and Accuracy. All isotherms were measured twice to ensure data precision. Replicate columns were treated as one data set when determining Freundlich coefficients. The 95% confidence intervals for Freundlich model fits were calculated. To ensure data accuracy, mass balances were performed by comparing the amount of TCE sorbed during column breakthrough to the amount of TCE desorbed during column elution. For the 15 °C columns, greater than 88% of the mass was recovered on desorption. For the 60 °C columns, recoveries ranged from 60% to 85%. Solids were autoclaved prior to use so no biodegradation is expected. Hydrolysis was neglected because the TCE half-life for this reaction is on the order of thousands of years at 60 °C (*48*). Thus, TCE is believed to be lost from these columns when they were uncapped and added to or removed from the purge apparatus.

TABLE 1. Physical Properties of Adsorbents Used

solid	$K_{F,aq}$[a] [$(\mu g/g)/(\mu g/mL)^{1/n}$]	1/n[a] (−)	N_2 surface area[b] (m^2/g)	$f_{oc}/^*f_{oc}$ (%/%)	water loading 15/60 °C[c] (mL/g)	particle diameter[d] (μm)	mesoporosity (mL/g)	median mesopore diameter[e] (Å)	air/water interfacial area to water vol[f] (m^2/g)	microporosity[g] (mL/g)
silica gel	15	0.61	297	<0.001/1.4	0.900 ± 0.008/ 0.890 ± 0.015	330[h]	0.76	60	0.004	0.1088
Santa Clara sediment	10	0.34	12	0.15/0.06	0.040 ± 0.001/ 0.040 ± 0.015	240	0.06	65	0.006	<0.0001
Norwood soil	2.9	0.79	55	1.4/0.26	0.140 ± 0.005/ 0.150 ± 0.015	220	0.145	65	0.007	<0.0001
Livermore sand fraction	0.44	0.54	13	0.064/0.063	0.041 ± 0.011/ 0.043 ± 0.005	150	0.54	69	0.010	<0.0001
Livermore clay and silt fraction	0.44	1.0	29	0.11/0.13	0.110 ± 0.021/ 0.089 ± 0.007	<75[i]	*j*	*j*	>0.020	<0.0001

[a] 30 °C values from Farrell and Reinhard (*5*). [b] BET method using nitrogen adsorption. [c] Values given are mean ± 95% CI and are calculated from the difference in column weight with solids at 100% RH and with solids baked dry. [d] Sauter mean diameter based on ASTM method. [e] Based on surface area using measured pore size distribution. [f] Air−water interfacial area calculated from particle diameter (assumed to be valid for primarily mesoporous solids here). [g] From Micromeritics of Norcross, CA, using Horvath and Kawazoe method and argon adsorption (*40*). [h] Monodisperse size distribution. [i] Measured properties not representative of moist solids due to swelling clays.

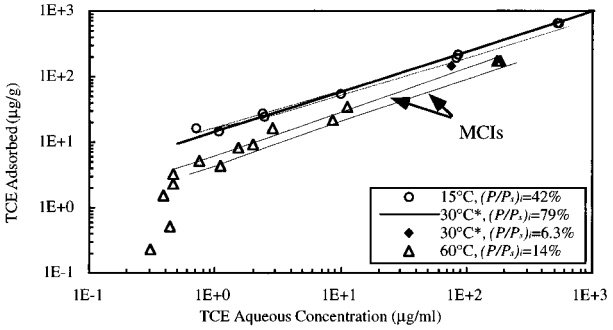

FIGURE 1. 15, 30, and 60 °C aqueous phase isotherms for TCE adsorbed to silica gel at 100% RH. 15 and 60 °C modified 95% confidence intervals are shown with their respective data sets (* indicates that it is from Farrell and Reinhard (*5*)).

Mass recovery was poorer at 60 °C than at lower temperatures because TCE diffused out of the columns faster at this temperature.

At each purge point $K_v(q_v) = q_v/C_{vap}$ was calculated. The value of C_{vap} was measured directly, and the value of q_v was calculated from the total mass removed during the current and all subsequent purges minus the vapor phase mass. Adding and removing columns from the purge apparatus took around 30 s, and mass lost errors may have affected $K_v(q_v)$ in two ways: (a) TCE lost from the vapor phase was not added to q_v in the previous purge point and (b) TCE lost from the vapor phase resulted in a C_{vap} that was not in equilibrium with q_v. Assuming that the percent of vapor phase mass lost during each purge point was the same, the mass lost at each purge point was calculated. Maximum possible errors in C_{vap} and q_v were calculated from these values, and the 95% confidence intervals were adjusted accordingly. The intervals plotted below are the modified 95% confidence intervals (MCIs) and account for both the precision and the mass lost errors. In almost all cases, MCIs are smaller or of the same size as the data symbols.

Results

Silica Gel. Figure 1 shows the replicate column data points and MCIs for aqueous phase TCE uptake on silica gel at 15 and 60 °C and the 30 °C isotherm calculated from the reported Freundlich parameters in Table 1. The MCIs at 60 °C are calculated from the log−log linear isotherm region. The MCIs at 30 °C are not available but are assumed to be similar to those at 15 °C. The 30 °C isotherm extends over the measured data range. The initial relative vapor pressures, $(P/P_s)_i$, for the different isotherms range from 14% at 60 °C to 79% at 30 °C. One additional equilibrium point is given at 30 °C to evaluate the effects of hysteresis. The $(P/P_s)_i$ for this point, 6.3%, is lower than $(P/P_s)_i$ for the 30 °C isotherm, 79%.

The 30 °C equilibrium point is slightly lower than the 30 °C isotherm, suggesting that hysteresis effects are small (i.e., on the order of MCIs). The 15 and 30 °C MCIs are coincident and above the 60 °C MCIs. The $1/n$ values at 15 and 60 °C, reported for all solids in Table 2, are not statistically different. The 60 °C isotherm is characterized by a Freundlich region and a region of data points that deviate from log−log linear behavior at low concentrations. The region where the amount adsorbed drops sharply from log−log linear behavior with decreasing aqueous phase concentration is designated the "non-Freundlich region". Such non-Freundlich behavior has been observed for benzene adsorption on charcoal (*49*). We are not aware of any studies where this behavior has been observed for organic chemical sorption on soils and sediments at 100% RH.

In the Freundlich isotherm region, $Q_{st}(q)$ values can be calculated from different temperature isotherms with eq 6. Small hysteresis effects and overlapping MCIs make isotherms separated by greater temperatures more amenable to $Q_{st}(q)$ calculations. Values of $Q_{st}(q)$ calculated from 15 and 60 °C MCIs are exothermic and are between 9.2 and 45 kJ/mol. Since values of $1/n$ are not statistically different at 15 and 60 °C, $Q_{st}(q)$ is constant for all q values.

In the non-Freundlich isotherm region, $Q_{st}(q)$ values cannot be calculated because 15 and 30 °C isotherms were not measured at similar q values due to detection limitations. If the 15 °C or the 30 °C isotherm continued to obey Freundlich behavior in this region, $Q_{st}(q)$ values would increase dramatically with decreasing sorbed phase concentration. Evidence for such behavior will be shown for the Livermore clay and silt fraction below.

Natural Solids. Aqueous phase isotherms for the two natural solids relatively high in organic matter ($f_{oc} > *f_{oc}$) are shown in Figure 2. The Santa Clara sediment isotherms are shown in Figure 2a. For this solid, the 30 °C equilibrium value with $(P/P_s)_i = 1.9\%$ is more than a factor of 2 below the 30 °C isotherm with $(P/P_s)_i = 65\%$. Also, the 30 °C isotherm is above the 15 °C isotherm, which is above the 60 °C isotherm, and $1/n$ values increase from 15 to 30 to 60 °C. The Norwood soil isotherms are shown in Figure 2b. For this solid, the 30 °C equilibrium value with $(P/P_s)_i = 6.4\%$ is below the 30 °C isotherm with $(P/P_s)_i = 43\%$. Also, the 15 and 30 °C isotherms are coincident, and $1/n$ values are not statistically different. Isotherms were not measured for the Norwood soil at 60 °C. At 60 °C significant amounts of soil organic matter volatilized and prevented accurate measurement of TCE.

The effect of $(P/P_s)_i$ on the 30 °C data in Figure 2 suggests that hysteresis effects are significant (i.e., exceed MCIs) in both cases, especially for the Santa Clara sediment. Here, the amount sorbed at the q value corresponding to the 30 °C equilibrium point increases with increasing $(P/P_s)_i$ but not necessarily with temperature. Thus, $(P/P_s)_i$ affects isotherm position more than temperature, suggesting that the $Q_{st}(q)$ value at this aqueous phase concentration is near zero. Below this sorbed phase concentration, the effects of $(P/P_s)_i$ were not measured. If $(P/P_s)_i$ only affects the position and not the slope of an isotherm, temperature is responsible for the observed increase in $1/n$ values with increasing temperature. As a result, $Q_{st}(q)$ values become greater at lower concentrations.

Hysteresis effects for the Norwood soil are less than for the Santa Clara sediment. For the Norwood soil, the 30 °C equilibrium value lies just outside the lower MCI of the 15 °C isotherm. Hence, changes in isotherm position due to $(P/P_s)_i$ do not significantly affect $Q_{st}(q)$. Values of $Q_{st}(q)$ calculated from the 15 and 30 °C isotherms are not statistically different from zero.

Aqueous phase isotherms for the Livermore sand and clay and silt fractions are shown in Figure 3, panels a and b, respectively. At 60 °C, Freundlich and non-Freundlich regions are present in both solids. Freundlich regions are evaluated first. For the sand fraction, the 60 and 30 °C MCIs overlap, the 30 and 15 °C MCIs overlap, and the 60 °C MCIs are slightly above the 15 °C MCIs. Hysteresis is not expected to affect sorption because the 60 °C isotherm with $(P/P_s)_i = 13\%$ is above the 15 °C isotherm with $(P/P_s)_i = 46\%$. Values of $1/n$ at all temperatures are not statistically different. For the clay and silt fraction, the 30 °C equilibrium value lies on the extension of the 30 °C isotherm, suggesting that hysteresis effects are insignificant. The three different temperature isotherms cross around 2 μg/mL, causing the 30 and 60 °C isotherms to shift relative positions. Values of $1/n$ for the Livermore clay and silt fraction increase from 60 to 15 to 30 °C.

Livermore sand fraction $Q_{st}(q)$ values can be calculated from the different temperature isotherms. The MCIs mask temperature effects between the 60 and 30 °C isotherms and between the 30 and 15 °C isotherms. Values of $Q_{st}(q)$

TABLE 2. Vapor Phase and Aqueous Phase Freundlich Isotherm Parameters at 15 and 60 °C[a]

	temp, T (°C)	$1/n_v$[b] (−)	$K_{F,v}$[c] [(μg/g)/(μg/ml)$^{1/n}$]	$1/n$[b] (−)	$K_{F,aq}$[c] [(μg/g)/(μg/ml)$^{1/n}$]
silica gel	15	0.67 ± 0.05	41	0.59 ± 0.04	15
	60	0.87 ± 0.13	3.03	0.66 ± 0.07	5.6
Santa Clara sediment	15	0.33 ± 0.02	14	0.27 ± 0.02	10
	60	0.48 ± 0.04	3.0	0.45 ± 0.04	3.7
Norwood soil	15	0.73 ± 0.05	9.38	0.70 ± 0.06	3.1
Livermore sand fraction	15	0.78 ± 0.07	0.77	0.65 ± 0.09	0.20
	60	0.65 ± 0.10	0.49	0.60 ± 0.10	0.57
Livermore clay and silt fraction	15	0.80 ± 0.10	1.4	0.71 ± 0.13	0.33
	60	0.55 ± 0.08	0.87	0.32 ± 0.08	0.79

[a] The 60 °C parameters are calculated from log−log linear isotherm regions. [b] Mean ± 95% confidence intervals are shown. [c] Confidence intervals on K_F are a function of the units used. Therefore, only mean values are shown.

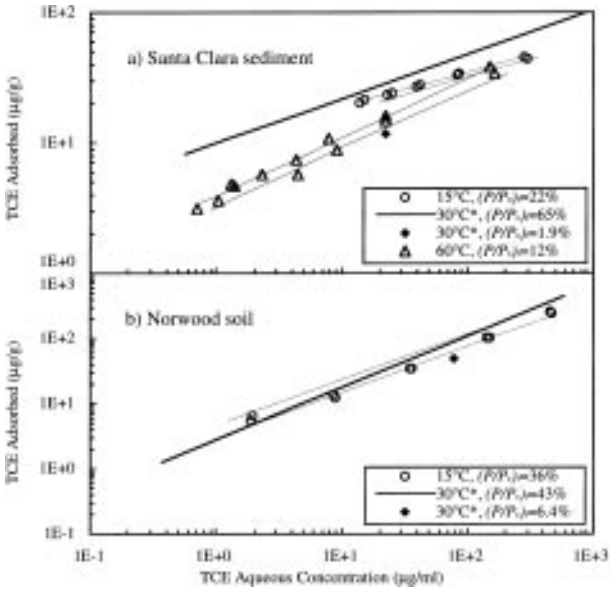

FIGURE 2. 15, 30, and/or 60 °C aqueous phase isotherms for TCE adsorbed to (a) Santa Clara sediment and (b) Norwood soil; all at 100% RH. 15 and 60 °C modified 95% confidence intervals are shown with their respective data sets (* indicates that it is from Farrell and Reinhard (*5*)).

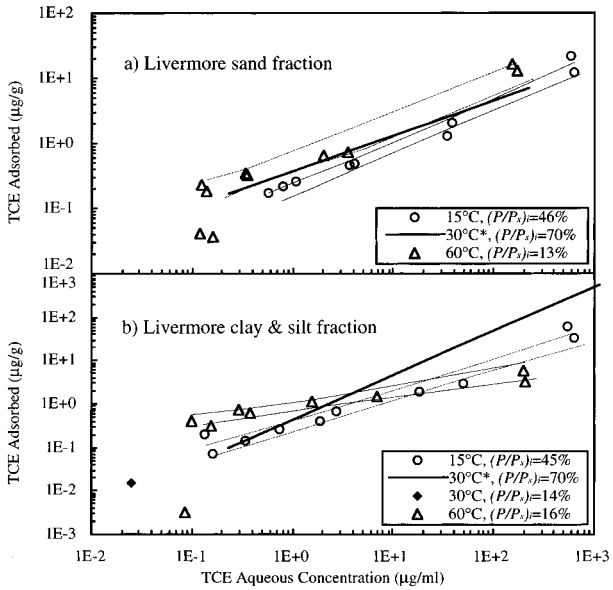

FIGURE 3. 15, 30, and 60 °C aqueous phase isotherms for TCE adsorbed to (a) the Livermore sand fraction and (b) the Livermore clay and silt fraction; all at 100% RH. 15 and 60 °C modified 95% confidence intervals are shown with their respective data sets (* indicates that it is from Farrell and Reinhard(*5*)).

calculated from the 60 and 15 °C MCIs are endothermic and range from zero to −13 kJ/mol. Livermore clay and silt fraction $Q_{st}(q)$ values could be calculated from the different temperature isotherms. Because the isotherms cross and because the vertical positions of the isotherms are not in order of increasing or decreasing temperature, the sign of $Q_{st}(q)$ would be a function of the two different temperature isotherms chosen.

In non-Freundlich regions, $Q_{st}(q)$ values cannot be calculated for the Livermore sand fraction. However, like the silica gel, if the 15 or 30 °C isotherm continues to obey Freundlich behavior at similar q values, $Q_{st}(q)$ values will increase sharply below 0.1 μg/g. For the Livermore clay and silt fraction, the 30 °C equilibrium value can be used with the corresponding the 60 °C isotherm value to calculate the $Q_{st}(q)$ value in the non-Freundlich region. A value of 34 kJ/mol is determined.

Discussion

Calculated $Q_{st}(q)$ values for silica gel are strongly exothermic (9.2 to 45 kJ/mol) and in the range expected for adsorption in micropores (*38*). Published data suggest that micropores are hydrophobic if aqueous phase organics adsorb in them (*35, 36*). Silica gel surfaces are largely hydrophilic (*50*); but they also exhibit some hydrophobic properties (*51*). Comparison of the maximum volume of TCE adsorbed (<0.2 μL/g) from Figure 1 to the total micropore volume (0.1088 mL/g) in Table 1 reveals that, if all uptake took place in micropores, less than 0.2% of the total micropore volume in silica gel would be occupied by TCE. Perhaps this small fraction of micropores is hydrophobic.

Values of $Q_{st}(q)$ at or near zero for the Santa Clara sediment and Norwood soil are consistent with sorption on water wet mineral surfaces (*12, 34*) or in AOM (*34*). Given that $f_{oc} > {}^*f_{oc}$ for these solids, sorption in AOM likely controls uptake when $Q_{st}(q)$ values are low. For the Santa Clara sediment, $Q_{st}(q)$ values appear to increase with decreasing concentration. This is consistent with a greater fraction of overall sorption occurring in micropores with decreasing concentration (*39*) and with the assumption that uptake in micropores is energetically favored over sorption in AOM.

As with the Santa Clara sediment and Norwood soil, values of $Q_{st}(q)$ in the Freundlich region for the Livermore sand fraction are consistent with sorption on water wet mineral surfaces or in AOM. Hysteresis effects are observed for the Santa Clara sediment and Norwood soil but not for the Livermore sand fraction where $f_{oc} \sim {}^*f_{oc}$. This suggests that (i) hysteresis is associated with AOM in these two cases and (ii) low $Q_{st}(q)$ values for the Livermore sand fraction are due to sorption on water wet mineral surfaces. Furthermore, hysteresis effects are more pronounced for the Santa Clara sediment than for the Norwood soil, but the later has a higher f_{oc}. Thus, hysteresis effects may be a function of both AOM content and type.

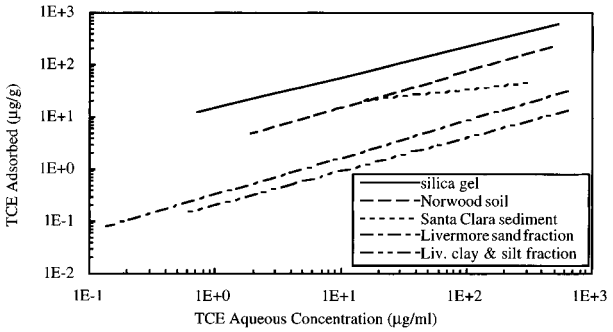

FIGURE 4. Comparison of silica gel, Livermore clay and silt fraction, Livermore sand fraction, Santa Clara sediment, and Norwood soil 15 °C aqueous phase Freundlich isotherms.

Values of $Q_{st}(q)$ in the Freundlich region for the Livermore clay and silt fraction are endothermic or exothermic depending on the pair of isotherms chosen. This behavior is not consistent with any of the mechanisms considered in this paper. Two possible explanations appear possible: (1) adsorption at the air−water interface is significant and temperature dependent and (2) adsorption on water wet clay mineral surfaces results in the observed behavior. Sorption mechanisms cannot be further inferred because of the inability to negate the first possibility.

Non-Freundlich behavior is observed for the silica gel and the Livermore solids. In all cases the 60 °C isotherm diverges from the 15 and 30 °C isotherms, suggesting that $Q_{st}(q)$ values increase sharply in this region. For the Livermore clay and silt fraction, a value of 34 kJ/mol is determined in the non-Freundlich region. This value is consistent with adsorption in hydrophobic micropores (*38*), the expected mechanism of uptake in the non-Freundlich regions.

Comparison of 15 °C Aqueous Phase Isotherms. The 15 °C Freundlich isotherms for the silica gel and four natural solids are compared in Figure 4. The silica gel isotherm is above all other isotherms. At high concentrations, the Norwood soil isotherm is above all others but the silica gel. As concentrations drop, the Norwood soil isotherm crosses the Santa Clara isotherm. The Livermore sand fraction and the Livermore clay and silt fraction isotherms are below all other isotherms. The observed isotherm positions mean that above 20 μg/mL $K_{aq}(q,\text{silica}) > K_{aq}(q,\text{Norwood}) > K_{aq}(q,\text{Santa Clara}) > K_{aq}(q,\text{Livermore solids})$ and below 20 μg/mL the ordering of $K_{aq}(q,\text{Norwood})$ and $K_{aq}(q,\text{Santa Clara})$ reverses.

Sorption in micropores is hypothesized to control uptake on the silica gel. The relative value of $K_{aq}(q,\text{silica})$ is consistent with adsorption in the highest energy sites. The f_{oc} value for the Norwood soil is ~10 times greater than for the other solids. At high concentrations, uptake on the natural solids is controlled by sorption in AOM and on water wet mineral surfaces, where the former is favored (*16*). Hence, the relative value of $K_{aq}(q,\text{Norwood})$ above 20 μg/mL is consistent with sorption in AOM. In the Santa Clara sediment, a greater fraction of overall sorption occurs in micropores with decreasing concentration. This is reflected by the change in ordering of $K_{aq}(q)$ values for the Santa Clara sediment and Norwood soil.

Modeling Non-Freundlich Adsorption. The Freundlich model is not capable of simulating log−log nonlinear behavior observed for some isotherms. To capture this sorption heterogeneity, a different form of the GAI (eq 4) is needed. For the silica gel, one $\theta_l(\epsilon_{aq})$ can be used to describe adsorption in micropores ($N = 1$). Ideally, $\phi(\epsilon_{aq})$ could be calculated from an independent measurement of the micropore width distribution and a micropore width to ϵ_{aq} relationship (*52, 53*). The function $\theta_l(\epsilon_{aq})$ could then be verified by the fit of the data. However, the micropore width distribution cannot be obtained, and $\phi(\epsilon_{aq})$ must be obtained by fitting the isotherm data.

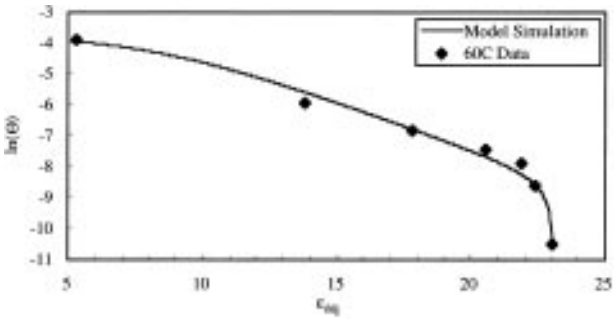

FIGURE 5. 60 °C aqueous phase isotherm and model simulation for TCE adsorbed to silica gel at 100% RH. Model simulation is general adsorption isotherm using local Langmuir isotherm with skewed log Gaussian adsorption free energy distribution.

The Langmuir equation is chosen to represent $\theta_l(\epsilon_{aq})$. A skewed log Gaussian function is used to represent $\phi(\epsilon_{aq})$ in eq 9.

$$\phi(\epsilon_{aq}) = \exp[-\ln(2)(\ln(1 + 2A(\epsilon_{aq} - \epsilon_{aq,m})/\sigma)/A)^2] \quad (9)$$

Polanyi's relationship, eq 10, is used to relate the relative aqueous phase concentration, $(C_{aq,s}/C_{aq})$, to ϵ_{aq} (*20*).

$$\epsilon_{aq} = RT \ln(C_{aq,s}/C_{aq}) \quad (10)$$

This relationship is widely used to predict the effects of T and $C_{aq,s}/C_{aq}$ on adsorption in micropores (*54, 55*). Upon integration of the GAI, the fit shown in Figure 5 is obtained. To arrive at this fit the width factor, σ, the skew factor, A, and the peak free energy of adsorption, $\epsilon_{aq,m}$, were optimized by minimizing the relative least squares of the model and experimental values (*56*).

In contrast to the silica gel, greater than one local isotherm is required to model sorption to soils and sediments. Fitting the GAI to isotherm data from these solids requires manipulating at least four adjustable parameters; no further effort is directed toward this end.

To predict isotherms, micropore size and hydrophobicity must be measured. Gas adsorption is currently used to measure micropore size. In the Santa Clara sediment, approximately 100 mg of TCE is adsorbed per gram of solid at the highest concentration measured. This amount is only 66% of the gas adsorption detection limit. The amounts of TCE sorbed in Livermore solid non-Freundlich regions are even smaller. Hence, gas adsorption techniques are not capable of measuring microporosity in natural solids.

No standard techniques are available to determine micropore hydrophobicity in natural solids. Previous authors have postulated that micropores are formed from mineral surfaces and hard organic matter (*13, 14*). Values of $Q_{st}(q)$ for the silica gel isotherms support the hypothesis that micropores are associated with mineral surfaces. Additional work is needed to determine if adsorption to hard organic carbon is characterized by large $Q_{st}(q)$ values. In the paper that follows (*57*), the effects of temperature on desorption kinetics are evaluated in light of the results presented in this paper.

Acknowledgments

Support for this work was provided by Lawrence Livermore National Laboratories (LLNL) through B209039 and the Environmental Protection Agency through R822626−01-0. The authors thank James Farrell of the University of Arizona for 30 °C isotherm data; George M. Deeley of Shell Development Co., Houston, TX, for the Norwood soil, and Dorothy Bishop of LLNL for her continued support. The content of

this paper does not necessarily represent the views of the supporting organizations.

Notation

A skew factor (−)

b Langmuir intensity coefficient (L^3/M_a)

C_{aq} aqueous phase concentration (M_a/L^3)

$C_{aq,s}$ aqueous phase concentration at the saturation limit of TCE (M_a/L^3)

f_{oc} fraction of organic carbon (M_{oc}/M_s)

$^*f_{oc}$ critical fraction of organic carbon (M_{oc}/M_s)

$\Delta G°$ change in standard Gibbs free energy [$M_aL^2/(t^2$ mol)]

H_c Henry's constant (C_v/C_{aq})

K general equilibrium distribution coefficient (−)

$K_{aq}(q)$ sorbed-aqueous equilibrium value at sorbed concentration q [$(M_a/M_s)/(M_a/L^3)$]

$K_{d,aq}$ sorbed-aqueous linear distribution coefficient [$(M_a/M_s)/(M_a/L^3)$]

$K_v(q_s)$ sorbed-vapor equilibrium value at sorbed concentration q_s [$(M_a/M_s)/(M_a/L^3)$]

$K_{F,aq}$ sorbed-aqueous Freundlich distribution coefficient [$(M_a/M_s)/(M_a/L^3)^{1/n}$]

$K_{F,v}$ sorbed-vapor Freundlich distribution coefficient [$(M_a/M_s)/(M_a/L^3)^{1/n}$]

K_{ow} octanol−water equilibrium distribution coefficient (−)

L length

M_a mass of adsorbate

M_{oc} mass of organic carbon

M_s mass of dry solids

N number of local isotherms (or mechanisms controlling sorption)

$1/n$ Freundlich exponent for aqeuous phase isotherm (−)

$1/n_v$ Freundlich exponent for vapor phase isotherm (−)

P vapor pressure (M_a/L^3)

P_s saturation vapor pressure (M_a/L^3)

Q_{st} isosteric heat of adsorption [$M_aL^2/(t^2$ mol)]

q concentration sorbed from the water to the soil or sediment grain (M_a/M_s)

q_l concentration sorbed from the water to the solid surface for a local isotherm (M_a/M_s)

$q_{l,s}$ final sorbed or adsorbed concentration for a local isotherm (M_a/M_s)

q_s final sorbed or adsorbed concentration (M_a/M_s)

q_v concentration sorbed from the vapor phase to the soil or sediment grain (M_a/M_s)

R ideal gas constant [$ML^2/(Tt^2$ mol)]

S surface area of solid (L^2/M_s)

T temperature (K)

t time

W_{sp} specific water content of a solid (L^3/M_s)

α constant (−)

ϵ_{aq} aqueous phase free energy of adsorption [$M_aL^2/(t^2$ mol)]

$\epsilon_{aq,m}$ peak aqueous phase free energy of adsorption [$M_aL^2/(t^2$ mol)]

$\phi(\epsilon_{aq})$ adsorption free energy distribution function (−)

Θ normalized overall isotherm (−)

$\theta_l(\epsilon_{aq})$ normalized local isotherm (q/q_0)

ρ_{TCE} liquid density of TCE (M_a/L^3)

σ Gaussian width factor [$M_aL^2/(t^2$ mol)]

Literature Cited

(1) Bucala, V.; Saito, H.; Howard, J. B.; Peters, W. A. *Environ. Sci. Technol.* **1994**, *28*, 1801−1807.
(2) Johnson, N. P.; Cosmos, M. G. *Pollut. Eng.* **1989**, *21*, 66−85.
(3) Ball, W. P.; Roberts, P. V. *Environ. Sci. Technol.* **1991**, *25*, 1223−1237.
(4) Ball, W. P.; Roberts, P. V. *Environ. Sci. Technol.* **1991**, *25*, 1237−1249.
(5) Farrell, J.; Reinhard, M. *Environ. Sci. Technol.* **1994**, *28*, 53−62.
(6) Farrell, J.; Reinhard, M. *Environ. Sci. Technol.* **1994**, *28*, 63−72.
(7) Grathwohl, P.; Reinhard, M. *Environ. Sci. Technol.* **1993**, *27*, 2360−2366.
(8) Pignatello, J. J. *Environ. Toxicol. Chem.* **1990**, *9*, 1107−1115.
(9) Fry, V. A.; Istok, J. D. *Water Resour. Res.* **1994**, *30*, 2413−2421.
(10) Gregg, S. J.; Singh, K. S. *Adsorption, Surface Area, and Porosity*; Academic Press: New York, 1982; pp 25−26.
(11) Chiou, C. T.; Shoup, T. D. *Environ. Sci. Technol.* **1985**, *19*, 1196−1200.
(12) Goss, K.; Eisenreich, S. J. *Environ. Sci. Technol.* **1996**, *30*, 2135−2142.
(13) Young, T. M.; Weber, W. J. J. *Environ. Sci. Technol.* **1995**, *29*, 92−97.
(14) Xing, B.; Pignatello, J. J.; Gigliotti, B. *Environ. Sci. Technol.* **1996**, *30*, 2432−2440.
(15) Garbarini, D. R.; Lion, L. W. *Environ. Sci. Technol.* **1986**, *20*, 1263−1269.
(16) Karickhoff, S. W.; Brown, D. S.; Scott, T. A. *Water Res.* **1979**, *13*, 241−248.
(17) Chiou, C. T.; Kile, D. E.; Malcolm, R. L. *Environ. Sci. Technol.* **1988**, *22*, 298−303.
(18) McCarty, P. L.; Reinhard, M.; Rittmann, B. E. *Environ. Sci. Technol.* **1981**, *15*, 40−51.
(19) Langmuir, I. J. *J. Am. Chem. Soc.* **1918**, *40*, 1361−1403.
(20) Ruthven, D. M. *Principles of Adsorption and Adsorption Processes*; John Wiley & Sons, Inc.: New York, 1984; pp 82−83.
(21) Pollard, S. J. T.; Thompson, F. E. *Water Res.* **1995**, *29*, 337−347.
(22) Adamson, A. W. *Physical Chemistry of Surfaces*, 5th ed.; John Wiley & Sons, Inc.: New York, 1990; pp 423−425.
(23) Jaroniec, M.; Madey, R. *Physical Adsorption On Heterogeneous Solids*; Elsevier Science and Publishing Co.: Amsterdam, 1988; pp 11−26.
(24) Freundlich, H. *Colloid and Capillary Chemistry*; E. P. Dutton & Company: New York, 1926.
(25) Grathwohl, P. *Environ. Sci. Technol.* **1990**, *24*, 1687−1693.
(26) McGinley, P. M.; Katz, L. E.; Weber, W. J. *Environ. Sci. Technol.* **1993**, *27*, 1524−1531.
(27) Weber, W. J.; McGinley, P. M.; Katz, L. E. *Environ. Sci. Technol.* **1992**, *26*, 1955−1962.
(28) Kan, A. T.; Fu, G.; Tomson, M. B. *Environ. Sci. Technol.* **1994**, *28*, 859−867.
(29) Seri-Levy, A.; Avnir, D. *Proceedings of the IVth International Conference on Fundamentals of Adsorption*, International Adsorption Society: Kyoto, 1992; pp 365−372.
(30) Bescmann, K.; Kokotailo, G. T.; Riekert, L. In *Characterization of Porous Solids*; Unger, K. K., Rouquerol, J., Sing, K. S. W., Kral, H., Eds.; Elsevier Science Publishers: Amsterdam, 1988; Vol. 39, pp 355−366.
(31) Blokzijl, W.; Engberts, J. B. F. N. *Angew. Chem. Int. Ed. Engl.* **1993**, *32*, 1545−1579.
(32) Hassett, J. J.; Banwart, W. L. In *Reactions and Movement of Organic Chemicals in Soils*; Sawhney, B. L., Brown, K., Eds.; Soil Science Society of America: Madison, WI, 1989; Vol. 22, pp 31−44.
(33) Ben-Naim, A. *J. Phys. Chem.* **1978**, *82*, 792−803.
(34) Noll, L. A. *Colloids Surf.* **1987**, *28*, 327−329.
(35) Weitkamp, J.; Ernst, S.; Gunzel, B.; Deckwer, W.-D. *Zeolites* **1991**, *11*, 314−317.
(36) Flanigen, E. M.; Bennett, J. M.; Grose, R. W.; Cohen, J. P.; Patton, R. L.; Kirchner, R. M.; Smith, J. V. *Nature* **1978**, *271*, 512−516.
(37) Pope, C. G. *J. Colloid Interface Sci.* **1987**, *116*, 221−223.
(38) Kaneko, Y.; Abe, M.; Ogino, K. *Colloids Surf.* **1989**, *37*, 211−222.
(39) Stach, H.; Lohse, U.; Thamm, H.; Schirmer, W. *Zeolites* **1986**, *6*, 74−90.
(40) Horvath, G.; Kowazoe, K. *J. Chem. Eng. Jpn.* **1983**, *16*, 470−475.
(41) Hirato, Y.; Nakasugi, O.; Yoshioka, M.; Sumi, K. *Water Sci. Technol.* **1992**, *25*, 9−16.

(42) Lesage, S.; Jackson, R. E.; Priddle, M. W.; Riemann, P. G. *Environ. Sci. Technol.* **1990**, *24*, 559−566.
(43) Olivieri, A. W.; Eisenberg, D. M.; Kurtovich, M. R.; Pettegrew, L. *J. Water Resour. Plan. Manage.* **1985**, *111*, 346−358.
(44) Gossett, J. M. *Environ. Sci. Technol.* **1987**, *21*, 202−208.
(45) Reklaitis, G. V. *Introduction to Material and Energy Balances*; John Wiley & Sons: New York, 1983; Appendix 4.
(46) Farrell, J. Ph.D. Thesis, Stanford University, 1993.
(47) Karger, B. L.; Castells, R. C.; Sewell, P. A.; Hartkopf, A. *J. Phys. Chem.* **1971**, *75*, 3870−3879.
(48) Jeffers, P. M.; Ward, L. M.; Woytowitch, L. M.; Wolfe, N. L. *Environ. Sci. Technol.* **1989**, *23*, 965−969.
(49) Heal, G. R. *Proceedings of the IVth International Conference* on Fundamentals of Adsorption; International Adsorption Society: Kyoto, 1992; pp 275−283.
(50) Scott, R. P. W. *Silica Gel and Bonded Phases*; John Wiley & Sons: New York, 1993; pp 71−95.
(51) Douillard, J. M.; Elwafir, M.; Partyka, S. *J. Colloid Interface Sci.* **1994**, *164*, 238−244.
(52) Dubinin, M. M. *Bull. Acad. Sci. USSR, Div. Chem. Sci.* **1979**, *28*, 1560−1564.
(53) Everett, D. H.; Powl, J. C. *J. Chem. Soc., Faraday. Trans. 1* **1976**, *72*, 619−636.
(54) Jaroniec, M.; Choma, J.; Burakiewicz-Mortka, W. *Carbon* **1991**, *29*, 1294−1296.
(55) Dubinin, M. M. *Carbon* **1989**, *27*, 457−467.
(56) Saez, P. B.; Rittmann, B. E. *Water Res.* **1992**, *26*, 789−796.
(57) Werth, C. J.; Reinhard, M. *Environ. Sci. Technol.* **1997**, *31*, 697−703.

Received for review March 13, 1996. Revised manuscript received October 29, 1996. Accepted October 29, 1996.[⊗]

ES9602307

[⊗] Abstract published in *Advance ACS Abstracts,* January 15, 1997.